

The Kinetics of Primary Events in the Reactions of $L_2Cu_2X_2$ Complexes (L is an N,N,N',N' -Tetraalkyldiamine; X is Cl or Br) with $M(NS)_2$ Reagents*

GEOFFREY DAVIES[†], NAGWA EL-KADY

Department of Chemistry, Northeastern University, Boston, Mass. 02115, U.S.A.

MOHAMED A. EL-SAYED, AHMED EL-TOUKHY[†]

Department of Chemistry, Faculty of Science, Alexandria University, Alexandria, Egypt

and MARK R. SCHURE[†]

Digital Equipment Corporation, Marlborough, Mass. 01752, U.S.A.

(Received December 21, 1987)

Abstract

The rate laws for the earliest events in the transmetalation of dimeric copper(I) complexes $L_2Cu_2X_2$ (L = N,N,N',N' -tetraalkyldiamine; X = Cl or Br) by $M(NS)_2$ reagents (M = Co, Ni, Cu, Zn; NS is a monoanionic *S*-methylhydrazinecarbodithioate Schiff base ligand) depend on L, X, M and NS and the aprotic solvent. The kinetic data are compared with those for monotransmetalation of copper(II) complexes $(\mu_4-O)N_4Cu_4X_6$ by $M(NS)_2$. Different kinetic behavior is particularly marked for cobalt(II) reactants. Unexpectedly high rates of reactions with $Cu(NS)_2$ are attributed to electron transfer. The results provide a basis for discussion of transmetalation specificity.

Introduction

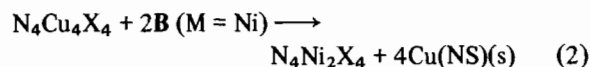
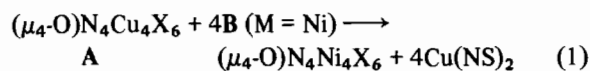
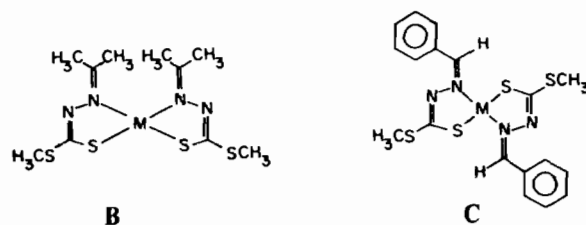
Transmetalation reactions are excellent, stoichiometric sources of heteropolynuclear metal complexes that cannot be obtained by other means [2–15].

Equations (1) [2–4, 7, 9, 12–14] and (2) [5, 15] are examples of stoichiometric transmetalation reactions. Here N is a monodentate pyridine, X is Cl or Br, NS is the monoanionic Schiff base ligand *S*-methylisopropylidenehydrazinecarbodithioate or *S*-methylbenzylidenehydrazinecarbodithioate and M is Co, Ni, Cu, Zn, Cd^{++} , Hg^{++} or Sn^{++} in $M(NS)_2$ reagents B or C, respectively.

*Taken in part from ref. 1.

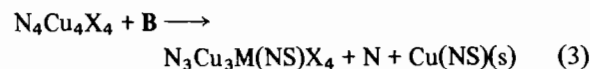
[†]Authors to whom correspondence should be addressed.

^{††}Even monotransmetalated species $(\mu_4-O)N_4CuMX_6$, (M = Cd, Hg and Sn) are unstable: the products are $(\mu_3-O)N_3Cu_3X_4$ trimers [16].

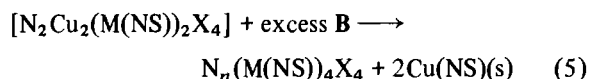
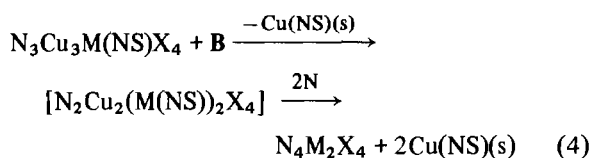


Reactions (1) proceed in four separate stoichiometric steps to give tetranuclear product families $(\mu_4-O)N_4Cu_{4-x}Ni_xX_6$ ($x = 0-4$) [7]. Each direct transmetalation step is driven by the formation of highly stable coproduct $Cu(NS)_2$. Reactions (1) occur on the stopped-flow timescale in aprotic solvents. Kinetic data for monotransmetalation ($x = 1$) of A with B and C (M = Co, Ni, Zn) indicate $\overline{Cu-X-M-S}$ ring formation between the reactants as a requirement for efficient metal exchange [5–9].

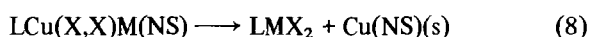
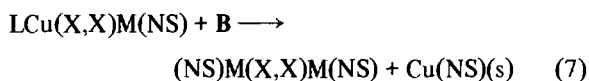
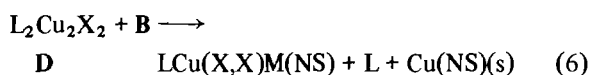
Reactions (2) proceed in two stoichiometric stages, eqns. (3) and (4), each of which is driven by formation of insoluble coproduct $Cu(NS)(s)$. Equation (3) is direct, but transmetalation of the stable primary product with B results in intramolecular NS ligand transfer from $M(NS)$ to copper(I), eqn. (4), which is not prevented by excess B, eqn. (5) [5, 15]. As a result, the total transmetalation of $N_4Cu_4X_4$ by B is not direct [5, 15]**.



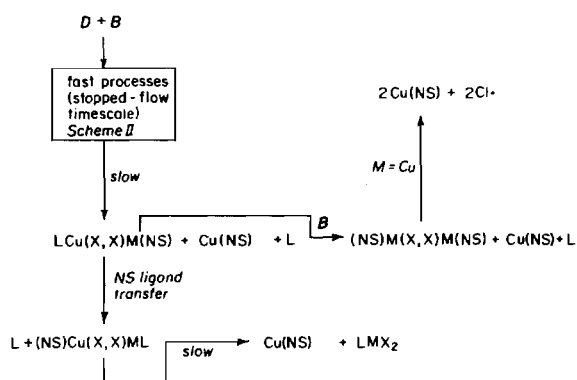
**Intramolecular NS ligand transfer is a common feature of progressive transmetalation of polynuclear copper(I) complexes [5, 8, 10, 15, 25].



Copper(I) complexes $L_2Cu_2X_2$ (**D**; L is an N,N,N',N' -tetraalkyldiamine) are of great interest because of their ability to initiate copper-catalyzed reactions of dioxygen [17]. Species **D** are halobridged dimers because of a preference for four-coordinate copper(I) [18–20]. Transmetalation reactions (6) and (7) are potential means of altering the efficiency and specificity of catalytic reactions, especially if M are redox-inactive. NS ligand transfer reaction (8) is a potential competitor of eqn. (7).



A recent study of the kinetics of $Cu(NS)(s)$ precipitation from eqns. (3), (4) and (6)–(8) in nitrobenzene with $L = N,N,N',N'$ -tetraethylethylenediamine showed that (i) $Cu(NS)(s)$ formation is very much slower than $Cu(NS)_2$ production in eqn. (1); (ii) that reactions (3) are rate-determining in the overall reactions of $N_4Cu_4X_4$ with excess **B**; and (iii) that the rates of reactions (6)–(8) increase in the order (8) < (6) < (7), Scheme 1 [15]. This



Scheme 1.

information ensures that the earliest events in reactions (6)–(8) do not refer to discrete $Cu(NS)(s)$ formation under any circumstances, which is the basis of the present work.

Here, we present a detailed comparison of (a) the kinetics of rapid monotransmetalation of **A** by **B** and **C** [4, 9] with (b) the kinetics of the earliest events in eqns. (6)–(8) and (c) the kinetics of the earliest reactions of **D** with **C**. This comparison shows that (a) the alkyl substituents and the bidentate character of the ligands L in **D** and (b) the nature of **B** and **C** play dominant roles in determining the rate law, the rate-determining step and the extent of reversibility in reactions of **D** with **B** and **C**. Differences in kinetic behavior are particularly sharp for reactions of **B** ($M = Co$), evidently because it is (a) nucleophilic but (b) tetrahedral and subject to inhibiting steric interactions with coordinated L. Unexpectedly high relative rates of irreversible reactions of **D** with **B** ($M = Cu$) are attributed to electron-transfer. The rate measurements provide a basis for discussion of monotransmetalation selectivity.

Experimental

Materials

Copper(I) chloride and copper(I) bromide were prepared by the literature method [21]. Procedures have been detailed for syntheses of $(ENCA)_4Cu_2Cl_2$ ($ENCA = \text{ethylnicotinate}$) [22], $L_2Cu_2X_2$ ($L = \text{TEED}$ or N,N,N',N' -tetrapropylethylenediamine, TPED (Alfa)) [15] and $M(NS)_2$ reagents **B** ($M = Co, Ni, Cu$) and **C** ($M = Ni$ or Cu) [23]. Solvents methylene chloride and nitrobenzene were purified as previously described [22].

Kinetic Measurements

Kinetic measurements were made in a custom-built stopped-flow spectrophotometer. Its flow system, made entirely of glass and quartz with fixed pathlength 3.3 mm, is immersed in a 5 l thermostat controlled to $\pm 0.02^\circ C$. The monitoring light beam passes in and out of the observation cell through quartz cones designed for total internal reflection, which makes the system sensitive to very small transmittance changes in chemical reactions. The spectrophotometric signal is measured with an RCA IP28VI photomultiplier run at ca. 300 V by a regulated DC power supply (Northeast Scientific Model PQE-1601). The resulting voltage is buffered by two unity gain operational amplifiers (Harris HA5130), whose inputs are connected in parallel. The output of one amplifier is fed to a storage oscilloscope (Tektronix 564B with 2A63 and 2B67 plug-ins) and the output of the other to a 16-bit A/D converter (Digital Equipment Corporation Model ADMPC-AA) controlled by a Digital Equipment Corporation Model PRO-350 personal computer. Data acquisition is activated by a microswitch on the stopping syringe. Switch closure triggers

the clock in the A/D converter, which controls the sampling rate. The switch closure contacts are debounced via a monostable circuit composed of an NE555 integrated circuit. Typically, 600 data points are collected for each experiment.

The data is stored on a 10 megabyte disk for processing. The processing step includes the visual display of absorbance and transmittance and the interactive determination of the parts of the absorbance curve to be used for the pseudo-first-order rate constant determination. The rate constant analysis is performed in the computer via a weighted least-squares fit of the quantity $\ln |A_\infty - A_t|$ versus time, where A_∞ is the absorbance at the end of the experimental run (the last six data points are averaged) and A_t is the absorbance at time t . Residual plots of the least-squares fits are then displayed as a quality check. All the software is run from a menu system using the P/OS version 2.0 operating system. All software is written in FORTRAN. See also 'Supplementary Material'.

Kinetic measurements were always made under pseudo-first-order conditions with one reagent in large excess. Specific conditions for each system are detailed in the following sections.

Results and Discussion

Equations (1)–(8) are stepwise, stoichiometric processes. The origin of the large driving forces in these reactions is the formation of especially stable $\text{Cu}(\text{NS})_2$ and $\text{Cu}(\text{NS})$ coproducts [2–15]. As a consequence, $\text{Cu}(\text{NS})_2$ is always the coproduct of polynuclear copper(II) transmetalation by $\text{M}(\text{NS})_n$ and the rate laws for rapid $\text{Cu}(\text{NS})_2$ product formation in the monotransmetalation of $(\mu_4\text{-O})[\text{NCu}]_4\text{X}_6$ complexes (**A**) by $\text{M}(\text{NS})_2$, eqn. (1), are those of irreversible rate-determining steps [4, 9].

We have established that polynuclear copper(I) sites ZCu^{I} are stoichiometrically transmetalated by $\text{Cu}(\text{NS})_2$ reagent **B** to leave $\text{Cu}(\text{NS})$ sites ZCu^{II} , eqn. (9) [5]. This indicates that $\text{Cu}(\text{NS})(\text{s})$ is even $\text{ZCu}^{\text{I}} + \text{B} (\text{M} = \text{Cu}) \longrightarrow \text{ZCu}^{\text{II}}(\text{NS}) + \text{Cu}(\text{NS})(\text{s})$ (9)

more stable than $\text{Cu}(\text{NS})_2$: as a consequence of an even larger driving force, the transmetalation of **D** by any $\text{M}(\text{NS})_2$ reagent **B** or **C** also should be governed by an irreversible rate law. However, the rate laws for transmetalation of **A** and **D** with fixed **B** or **C** might differ because bulky, bidentate **L** in **D** could impose different structural requirements than do monodentate **N** in **A** (Fig. 1).

Of relevance is our observation that the transmetalations of tetranuclear L_4Cu_4 and $\text{L}_4\text{Cu}_4\text{O}_2$ complexes ($\text{L} = 6\text{-methyl-2-oxopyridinate}$) are generally slower than those of tetranuclear halo(amine) copper complexes with a given $\text{M}(\text{NS})_2$ transmet-

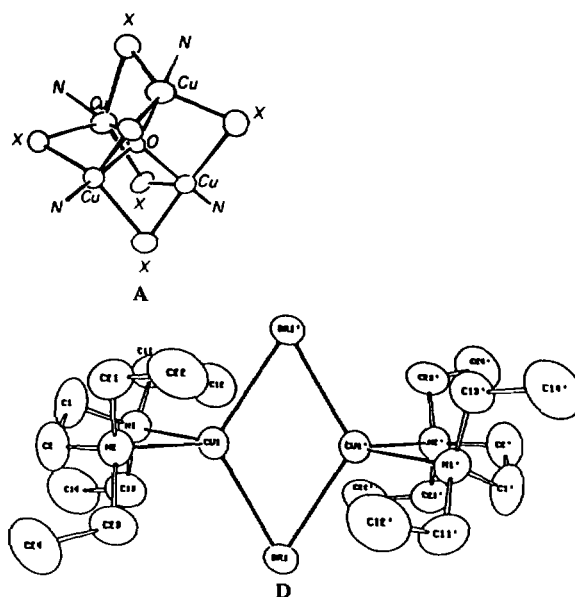


Fig. 1. Molecular structures of $(\mu_4\text{-O})[(\text{DENC})\text{Cu}]_4\text{X}_6$ (**A**) [2] and $(\text{TEED})\text{Cu}(\text{Br},\text{Br})\text{Cu}(\text{TEED})$ (**D**) viewed normal to the $\text{Cu}(\text{Br},\text{Br})\text{Cu}$ plane [19].

alator under the same experimental conditions [6, 24]. This strongly suggests that the accessible halogen atoms **X** in **A** and **D** (Fig. 1) are directly involved in their transmetalation [4, 9].

A review of factors in the kinetics of monotransmetalation of **A** is necessary before attempting to describe and interpret the corresponding data for **D**.

Kinetics of Monotransmetalation of **A** by **B** and **C**

We studied the kinetics of the title reactions with excess **A** to ensure monotransmetalation [4, 9]. Irreversible rate laws (10)–(12) were observed under these conditions (Table I).

$$d[\text{Cu}(\text{NS})_2]/dt = k_{10}[\text{B}][\text{A}]^2 \quad (10)$$

$$d[\text{Cu}(\text{NS})_2]/dt = k_{11}[\text{B}] \quad (11)$$

$$d[\text{Cu}(\text{NS})_2]/dt = k_{12}[\text{C}][\text{A}] \quad (12)$$

Third-order, irreversible rate law (10) was characteristic of **B** and is a clear indication of reactant preassociation [4]. Accessible **X** in **A** (Fig. 1) and nucleophilic carbothioate **S** in **B** [25–27] are considered to favor preassociation via two Cu-X-M-S rings to give species $\text{B}\cdot\text{A}_2$ [4]. However, rate law (10) indicates [9] that only weak precursors $\text{B}\cdot\text{A}_2$ are present and literature data [28]* for very fast

*The largest reported equilibrium constant for formation of $\text{Ni}(\text{NS})_2\cdot\text{P}_2$ complexes is $71 \pm 4 \text{ M}^{-2}$ in benzene at 25°C with $\text{NS} = S\text{-methyl-}p\text{-chloroarylidenhydrazinecarbodithioate}$ and $\text{P} = 4\text{-methylpyridine}$ [28]. We give the average and average deviation for the published data.

TABLE I. Kinetic Data for Rate Laws (10)–(12) [9]

X in A	Reagent, M	Solvent ^a			
Rate law (10)			k_{10} ^b	ΔH^\ddagger_{10} ^c	ΔS^\ddagger_{10} ^d
Cl ^e	B, Ni	NB	16200	20.0 ± 0.3	29 ± 3
Br ^e	B, Ni	NB	250	24.0 ± 0.4	35 ± 3
Cl ^{e, f}	B, Ni	NB	18900	20.4 ± 0.4	30 ± 3
Cl	B, Ni	MC	97000	16.5 ± 0.4	20 ± 3
Cl	B, Co	NB	860000	20.0 ± 0.4	36 ± 3
Cl	B, Co	MC	340000	19.5 ± 0.4	33 ± 3
Cl	B, Zn	NB	164000	20.0 ± 0.3	33 ± 3
Cl	B, Zn	MC	475000	14.0 ± 0.4	15 ± 3
Rate law (11)			k_{11} ^g	ΔH^\ddagger_{11} ^c	ΔS^\ddagger_{11} ^d
Br	B, Zn	NB	2.8	12.8 ± 0.4	–(13 ± 2)
Br	B, Zn	MC	0.85	17.0 ± 0.4	–(1 ± 2)
Br	B, Co	NB	0.52	18.0 ± 0.4	1 ± 2
Br	B, Co	MC	1.1	15.8 ± 0.4	–(5 ± 2)
Rate law (12)			k_{12} ^h	ΔH^\ddagger_{12} ^c	ΔS^\ddagger_{12} ^d
Cl ^e	C, Ni	NB	12.6	4.2 ± 0.3	–(38 ± 4)
Cl	C, Ni	MC	3.8	4.8 ± 0.3	–(39 ± 3)
Cl	C, Zn	NB	8700	8.5 ± 0.3	–(12 ± 2)
Br	C, Zn	NB	3900	21.2 ± 0.4	33 ± 3
Cl	C, Zn	MC	2100	9.7 ± 0.3	–(11 ± 2)
Br	C, Zn	MC	4000	17.7 ± 0.3	18 ± 3

^aNB = nitrobenzene, MC = methylene chloride. ^bUnits are $M^{-2} s^{-1}$ at 21 °C. ^cUnits are $kcal mol^{-1}$; error shown is 1 standard deviation. ^dUnits are $cal deg^{-1} mol^{-1}$ at 25 °C; error shown is 1 standard deviation. ^eData from ref. 4. ^fLigand in A is pyridine; all others have monodentate *N,N*-diethylnicotinamide as ligand. ^gUnits are s^{-1} at 21 °C. ^hUnits are $M^{-1} s^{-1}$ at 21 °C.

B·py₂ formation (py is a monodentate pyridine) suggest that **B**·**A** and **B**·**A**₂ are in rapid equilibrium, eqn. (13). We used the literature data [28] to assign



$\Delta S_{13} = -44 \pm 3 cal deg^{-1} mol^{-1}$. A steady-state treatment of the proposed mechanism then gave $\Delta S_{rds}^\ddagger = \Delta S_{10}^\ddagger + 44$, where ΔS_{10}^\ddagger is the observed entropy of activation and ΔS_{rds}^\ddagger is the activation entropy of the first-order rate-determining step [9]. Since ΔS_{10}^\ddagger are already markedly positive (Table I), we concluded that the formation of discrete reaction products after rapid metal exchange in **B**·**A**₂ was the first-order rate-determining step; product formation with **B** (M = Ni) has the lowest rate (Table I).

The other important features of the data for rate law (10) are that variations of N in **A** or solvent have little effect on k_{10} but that changing from X = Cl to X = Br in reactions of **A** with **B** (M = Ni) causes a dramatic decrease in k_{10} (Table I). Copper(I)–X bond breaking evidently is necessary for slow final product formation [9].

A different rate law (11) was observed for excess **A** (X = Br) reacting with **B** (M = Co or Zn) [9]. This phenomenon is important for two reasons.

First, it indicates that particularly nucleophilic X and S atoms and accessible metal centers can lead to strong interaction via $\overline{Cu-X-M-S}$ rings. Second, its interpretation requires no assumptions of ΔS_{13} or precursor stoichiometries. The data (Table I) exhibit $\Delta S_{11}^\ddagger \approx 0$, which is much more consistent with slow, first-order metal exchange in $\overline{Cu-Br-(Co,Zn)-S}$ rings than with slow fragmentation to final products. Slow metal exchange thus appears to be characteristic of particularly stable reaction precursors.

Second-order, irreversible rate law (12) was found to be characteristic of the monotransmetalation of **A** by **C** [4, 9]. No analogue of first-order rate law (11) was observed under similar conditions; the order of eqn. (12) indicates that **C**·**A**₂ are weaker species than **B**·**A**₂ (cf. eqn. (10)), presumably because the S atoms of **C** are less nucleophilic than those in **B** [25–27]. We assumed that eqn. (14) is a rapid



pre-equilibrium and assigned $\Delta S_{14} = -25 \pm 3 cal deg^{-1} mol^{-1}$ from the data for formation of **B**·bipy, where bipy is 2,2'-bipyridyl [28]. A steady-state treatment with the expectation that ΔS^\ddagger for metal exchange would be near zero (see above) then predicted that $\Delta S_{rds}^\ddagger = \Delta S_{12}^\ddagger + 25$. This treatment of

the experimental activation entropies ΔS_{12}^{\ddagger} (Table I) suggested [9] that first-order metal exchange in Cu-Cl-Ni-S rings is rate-determining in the mono-transmetalation of **A** ($X = \text{Cl}$) by **C** ($M = \text{Ni}$) by comparison with $\Delta S_{\text{rds}}^{\ddagger}$ derived from rate law (10). Activation entropies $\Delta S_{\text{rds}}^{\ddagger}$ are much more positive for the reactions of **A** ($X = \text{Br}$) with **C** ($M = \text{Zn}$), suggesting faster metal exchange and a later rate-determining step than with $M = \text{Ni}$. This is consistent with our observation that the stability order of $M(\text{NS})_2$ complexes decreases in the order $\text{Cu} \gg \text{Ni} \gg \text{Co} \gg \text{Zn}$ in ligand systems **B** or **C** [10]. On this basis Cu-Zn exchange should be faster than Cu-Ni exchange in Cu-X-Ni(Zn)-S rings, and discrete product formation becomes the slow first-order step in the reaction of **A** ($X = \text{Br}$) with **C** ($M = \text{Zn}$) [9].

The data for reaction of **A** ($X = \text{Cl}$) with **C** ($M = \text{Zn}$), Table I, are the most difficult to interpret since $\Delta S_{\text{rds}}^{\ddagger} \approx 13 \text{ cal deg}^{-1} \text{ mol}^{-1}$. If this is accepted to be too positive for rate-determining metal exchange we have a further indication that metal exchange is fastest with $M = \text{Zn}$ in Cu-Cl-M-S rings.

Summary

Differences in the irreversible rate laws for mono-transmetalation of **A** by **B** and **C** are due to involvement of different rapidly equilibrated species $\text{B}\cdot\text{A}_2$ and $\text{C}\cdot\text{A}$. Rate-determining first-order metal exchange can be recognized from $\Delta S_{11}^{\ddagger} \approx 0$ when $\text{B}\cdot\text{A}_2$ are especially stable and in weaker $\text{B}\cdot\text{A}_2$ species by accounting for the effect of reactant preassociation on ΔS_{10}^{\ddagger} . Faster metal exchange with weaker $M(\text{NS})_2$ causes a shift to rate-determining product formation, which can be recognized from markedly positive entropies of activation and a dramatic decrease in rate on changing from **A** ($X = \text{Cl}$) to **A** ($X = \text{Br}$) with **B** ($M = \text{Ni}$). On this basis, discrete product formation is the most common slow step in the mono-transmetalation of **A** by **B** and **C** (eqn. (1), $x = 1$) [9].

Kinetics of Fast Reactions of **D** with **B** and **C**. Experimental Conditions

The kinetics of rapid reactions of **D** with **B** and **C** were mostly studied under pseudo-first-order conditions with excess **D** to ensure ultimate mono-transmetalation and to allow direct comparison with the corresponding data for **A** [9]. A few systems were also studied with excess **B** ($M = \text{Ni}$) to examine the effect of this change on the rate law. We have demonstrated previously that mono-transmetalation also is rate-determining under these conditions [15].

Third-order, Irreversible Rate Laws for Transmetalation of Excess **D** and $(\text{ENCA})_4\text{Cu}_2\text{Cl}_2$ by **B**

The kinetics of rapid reactions of excess **D** ($L = \text{TEED}$ or TPED , $X = \text{Cl}$ or Br) and $(\text{ENCA})_4\text{Cu}_2\text{Cl}_2$,

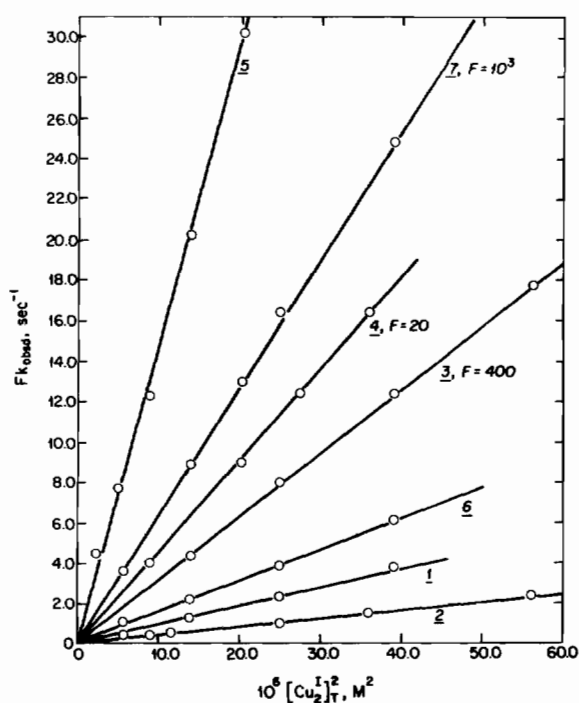


Fig. 2. Plots of $Fk_{\text{obs}} (\text{s}^{-1})$ vs. $[\text{Cu}^{\text{I}}]_{\text{T}}^2$ for the following systems in rate law (15): 1, $(\text{TEED})_2\text{Cu}_2\text{Cl}_2$ with **B** ($M = \text{Ni}$) in methylene chloride (MC) at 22.4 °C; 2, $(\text{TEED})_2\text{Cu}_2\text{Cl}_2$ with **B** ($M = \text{Ni}$) in nitrobenzene (NB) at 25.8 °C; 3, $(\text{TEED})_2\text{Cu}_2\text{Br}_2$ with **B** ($M = \text{Ni}$) in MC at 18.8 °C; 4, $(\text{TPED})_2\text{Cu}_2\text{Cl}_2$ with **B** ($M = \text{Ni}$) in NB at 21.7 °C; 5, $(\text{TEED})_2\text{Cu}_2\text{Cl}_2$ with **B** ($M = \text{Cu}$) in NB at 19.7 °C; 6, $(\text{TEED})_2\text{Cu}_2\text{Br}_2$ with **B** ($M = \text{Cu}$) in NB at 20.0 °C; 7, $(\text{ENCA})_4\text{Cu}_2\text{Cl}_2$ with **B** ($M = \text{Co}$) at 32.0 °C.

$(1.25-7.50) \times 10^{-3} \text{ M}$, by **B** ($M = \text{Co}, \text{Ni}, \text{Cu}$), $(1.0-2.0) \times 10^{-4} \text{ M}$, were investigated in methylene chloride (all ligands) and nitrobenzene (ligand not ENCA)* under dinitrogen. Absorbance monitored at 400–625 nm gave plots of $\ln(A_{\infty} - A_t)$ versus time, where A_t is absorbance at time t , which were linear to at least 4 half-lives, indicating a first-order dependence of the rate law on $[\text{B}]$. Plots of the observed pseudo-first-order rate constant at constant temperature, k_{obs} , versus $[\text{D}]^2$ were linear and passed through the origin, Fig. 2, indicating irreversible, third-order rate law (15). This high reaction order is indicative of reactant preassociation [9].

$$\text{rate} = k_{15} [\text{B}] [\text{D}]^2 \quad (15)$$

Third-order rate constants k_{15} and their associated activation parameters are collected in Table II (see also 'Supplementary Material'). Excess **D/B**

*ENCA forms tetranuclear complexes $[(\text{ENCA})\text{CuX}]_4$ and $[(\text{ENCA})_2\text{CuX}]_4$ with copper(I) halides CuX if the solvent is nitrobenzene under comparable experimental conditions [22].

TABLE II. Kinetic Data for Third-order Transmetalation of Excess **D** by **B** in Aprotic Solvents (eqn. (15))

Copper reactant D	M in B	Solvent ^a	$10^{-4} \times k_{15}$ ^b	ΔH^\ddagger_{15} ^c	ΔS^\ddagger_{15} ^d
(ENCA) ₄ Cu ₂ Cl ₂	Co	MC	0.048	2.1 ± 0.3	-(39 ± 3)
(TEED) ₂ Cu ₂ Cl ₂	Ni	MC	4.6	8.4 ± 0.3	-(9 ± 3)
		NB	4.0	8.9 ± 0.3	-(6 ± 3)
(TEED) ₂ Cu ₂ Br ₂		MC	0.083	20.0 ± 0.3	23 ± 3
(TPED) ₂ Cu ₂ Cl ₂		NB	2.3	13.4 ± 0.4	7 ± 3
(TEED) ₂ Cu ₂ Cl ₂	Cu	NB	174	9.6 ± 0.2	3 ± 3
(TEED) ₂ Cu ₂ Br ₂		NB	33.5	11.1 ± 0.3	4 ± 3

^aMC = methylene chloride, NB = nitrobenzene. ^bUnits are M⁻² s⁻¹ at 21 °C; typical precision = ± 5%. ^cUnits are kcal mol⁻¹. ^dUnits are cal deg⁻¹ mol⁻¹ at 25 °C.

systems which do not obey rate law (15) under the same experimental conditions are considered in a later section.

Features of the Kinetic Data for Rate Law (15)

All **A** and **D** have accessible X atoms (Fig. 1) and most are transmetalated by **B** with third-order rate laws (10) and (15) when **A** or **D** is in excess. It therefore is appropriate to compare the respective data.

Commonalities in the Kinetic Data with **B** (M = Ni)

Transmetalation of **A** and **D** by **B** (M = Ni) is third-order (eqn. (10) or (15)). Changing N (in **A**), L (in **D**) or solvent with X = Cl has little effect on k_{10} or k_{15} , which have similar magnitudes. However, changing X from Cl to Br causes a dramatic decrease in either of the respective third-order rate constants.

Cobalt and Zinc Data

Comparison of data for transmetalation of **A** and **D** by **B** (M = Co or Zn) is restricted because of changes of rate law (*vide infra*). Thus, rate law (10) is obeyed in the transmetalation of **A** (X = Cl) by **B** (M = Co or Zn) but changing X = Cl to Br gives rate law (11) [9]. Although we could not find a suitable monitoring wavelength for the reactions of **D** with **B** (M = Zn), we did find that none of the data for **B** (M = Co) fit rate law (15) despite the fact that rate law (10) is obeyed with **A** (X = Cl): the data for **D** (X = Br) fit second-order rate law (16) and with X = Cl the observed reaction actually is reversible (see below). However, third-order behavior, eqn. (15), was observed for transmetalation of (ENCA)₂Cu₂Cl₂ by **B** (M = Co) (Table II), indicating that rate law changes for **D** are ligand-induced and dependent on M(NS)₂ geometries [23] (see below).

Copper(II) Data

We observe that k_{15} is highest for reaction of **D** (L = TEED, X = Cl) with **B** (M = Cu) despite the fact that this is by far the most thermodynamically

stable of the **B** transmetalators [10]. Also notable is that the effect of changing X = Cl to Br in **D** on k_{15} is much smaller for **B** (M = Cu) than for **B** (M = Ni), Table II.

Activation Parameter Correlation

Observed activation parameters ΔH^\ddagger and ΔS^\ddagger for transmetalation are less positive when the reactant is **D**. However, we noticed that respective ΔH^\ddagger and ΔS^\ddagger for rate laws (10) and (15) appear to be correlated and found that a plot of ΔH^\ddagger_{10} versus ΔS^\ddagger_{10} and ΔH^\ddagger_{15} versus ΔS^\ddagger_{15} gave a common straight line (not shown) for all the data in Tables I and II. This correlation suggests similar structural features in systems governed by third-order rate laws (see below).

Second-Order Rate Laws for Fast Reactions of **A** and **D** with **B** and **C**. General Observations

In this and the next eight sections we describe forward processes which are first-order in [**A**] or [**D**] and first-order in [**B**] or [**C**].

Our previous work shows that the rate law for transmetalations of excess **A** by **C** (M = Ni or Zn) in methylene chloride and nitrobenzene is first-order in [**A**] and first-order in [**C**], eqn. (12), which differs from rate law (10) for the majority of reactions with **B** under similar experimental conditions [9].

Second-order behavior, eqn. (16), was observed in corresponding reactions of **D** and thus appears

$$\text{rate} = k_{16}[\text{C}][\text{D}] \quad (16)$$

to be characteristic of transmetalators **C**. We also found that reaction of **D** (X = Br) with **B** (M = Co) is second-order (eqn. (16): **B** replaces **C**) even with excess **D** and is reversible with **D** (X = Cl) (see below).

Systems which obey second-order forward rate laws were identified from the following results.

Reactions of Excess **D** with **C** (M = Ni)

The kinetics of monotransmetalations of excess **D**, (2.5–7.5) × 10⁻³ M, by **C** (M = Ni), (1.0–2.0) ×

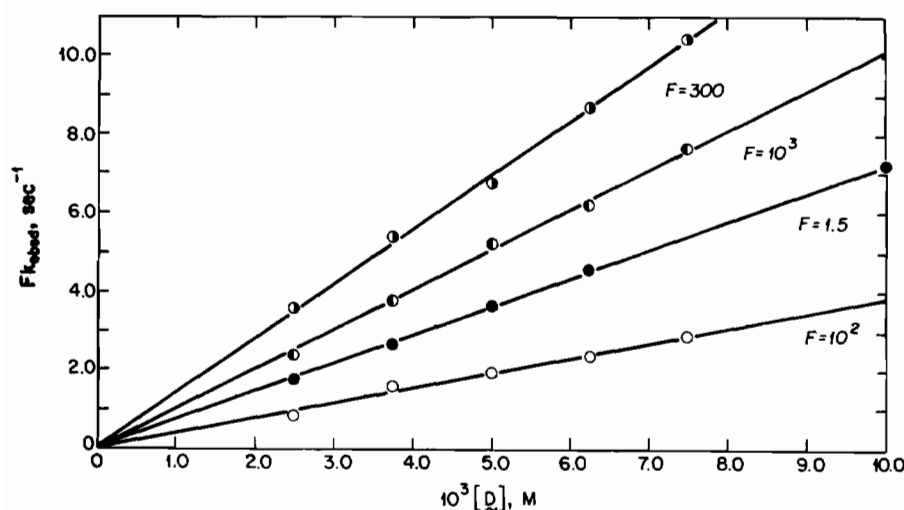


Fig. 3. Plots of Fk_{obs} (s^{-1}) vs. $[\text{D}]$ for the following systems in rate law (16): \circ , $(\text{TEED})_2\text{Cu}_2\text{Cl}_2$ with **C** ($\text{M} = \text{Ni}$) in methylene chloride (MC) at 19.6°C ; \bullet , $(\text{TEED})_2\text{Cu}_2\text{Cl}_2$ with **C** ($\text{M} = \text{Ni}$) in nitrobenzene (NB) at 33.6°C ; \circ , $(\text{TEED})_2\text{Cu}_2\text{Br}_2$ with **C** ($\text{M} = \text{Ni}$) in MC at 31.0°C ; \bullet , $(\text{TEED})_2\text{Cu}_2\text{Br}_2$ with **B** ($\text{M} = \text{Co}$) in NB at 32.3°C .

TABLE III. Kinetic Data for Second-order Transmetalation of **D** by **B** and **C** in Aprotic Solvents (eqns. (16) and (17))

Copper reactant	B or C , M	Solvent ^a	k_{16} ^b	ΔH_{16}^\ddagger ^c	ΔS_{16}^\ddagger ^d
Data for rate law (16)					
$(\text{TEED})_2\text{Cu}_2\text{Cl}_2$	B , Ni ^e	NB	17.8	20.4 ± 0.4	16 ± 3
$(\text{TEED})_2\text{Cu}_2\text{Br}_2$		MC	55.0	20.2 ± 0.4	18 ± 3
		NB	6.0	26.2 ± 0.4	34 ± 3
$(\text{TEED})_2\text{Cu}_2\text{Br}_2$ ^e	B , Co	NB	251	9.6 ± 0.4	$-(15 \pm 3)$
$(\text{TEED})_2\text{Cu}_2\text{Cl}_2$ ^e		MC	530	9.5 ± 0.4	$-(14 \pm 3)$
	C , Ni	MC	0.74	16.2 ± 0.3	$-(4 \pm 3)$
		NB	0.26	18.4 ± 0.4	1 ± 3
$(\text{TEED})_2\text{Cu}_2\text{Br}_2$ ^e		MC	2.0	17.8 ± 0.3	3 ± 3
Data for forward rate law (17)					
$(\text{TEED})_2\text{Cu}_2\text{Cl}_2$ ^e	C , Cu	NB	1740	11.3 ± 0.4	$-(5 \pm 2)$
$(\text{TEED})_2\text{Cu}_2\text{Br}_2$ ^e	B , Co	NB	370	10.6 ± 0.3	$-(11 \pm 2)$
	C , Cu	NB	470	13.9 ± 0.3	1 ± 2

^aNB = nitrobenzene, MC = methylene chloride. ^bUnits are $\text{M}^{-1} \text{s}^{-1}$ at 21°C . ^cUnits are kcal mol^{-1} . ^dUnits are $\text{cal deg}^{-1} \text{mol}^{-1}$ at 25°C . ^eDesignates reactant in excess. ^fForward parameters for reversible rate law (17) (see text).

10^{-4} M, were investigated in methylene chloride and nitrobenzene under dinitrogen. Absorbances monitored at 400–425 nm under pseudo-first-order conditions gave plots of $\ln(A_\infty - A_t)$ versus time which were linear for at least 4 half-lives, indicating a first-order dependence of the rate law on $[\text{C}]$. Plots of the observed pseudo-first-order rate constants at fixed temperature, k_{obs} , versus $[\text{D}]$ were linear and passed through the origin, Fig. 3, indicating second-order rate law (16). Second-order rate constants k_{16} and their associated activation parameters are collected in Table III (see also 'Supplementary Material').

Reactions of **D** with Excess **B** ($\text{M} = \text{Ni}$)

In an earlier paper we demonstrated that the reactions of **D** with excess **B** ($\text{M} = \text{Ni}$) in nitrobenzene proceeds via rate-determining step S1, Scheme 1 [15]. We could thus investigate the kinetics of monotransmetalation of **D** ($\text{X} = \text{Cl}$ and Br), 2.0×10^{-4} M, with excess **B** ($\text{M} = \text{Ni}$), $(2.0\text{--}5.0) \times 10^{-3}$ M, in methylene chloride and nitrobenzene under dinitrogen. Absorbances monitored at 480 nm gave plots of $\ln(A_\infty - A_t)$ versus time which were linear to at least 4 half-lives, indicating a first-order dependence on $[\text{D}]$. Plots of the pseudo-first-order rate constants at fixed temperature, k_{obs} , versus

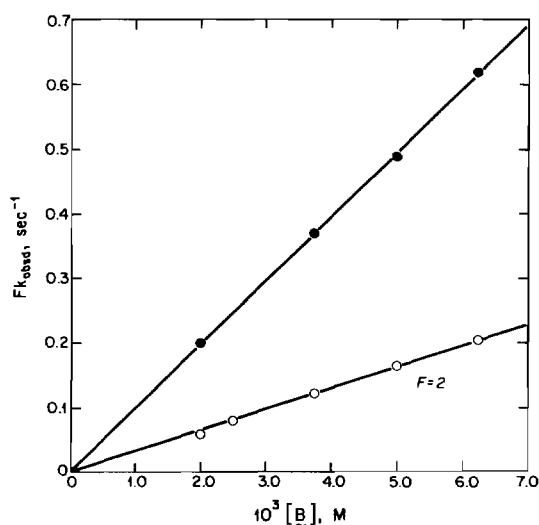


Fig. 4. Plots of Fk_{obs} (s^{-1}) vs. $[\text{B}]$ for the following systems in rate law (16): \circ , **B** ($M = \text{Ni}$) with $(\text{TEED})_2\text{Cu}_2\text{Cl}_2$ in nitrobenzene (NB) at 20.0°C ; \bullet , **B** ($M = \text{Ni}$) with $(\text{TEED})_2\text{Cu}_2\text{Br}_2$ in methylene chloride (MC) at 22.5°C .

excess $[\text{B}]$ were linear and passed through the origin (Fig. 4), indicating second-order rate law (16) with **B** ($M = \text{Ni}$) replacing **C**. This rate law differs from third-order rate law (15) observed with excess **D** and shows the effect of decreasing $[\text{D}]$ on the stoichiometry of species involved in monotransmetalation by **B** (see below). Kinetic data are collected in Table III (see also 'Supplementary Material').

Reaction of Excess **D** ($X = \text{Br}$) with **B** ($M = \text{Co}$)

The kinetics of reaction of excess **D** ($X = \text{Br}$ but not Cl , see below), $(2.5\text{--}6.3) \times 10^{-3}$ M, with **B** ($M = \text{Co}$), 2.0×10^{-4} M, monitored at 625 nm in nitrobenzene also were found to obey rate law (16) (**B** replaces **C**) and not rate law (15). Kinetic data are presented in Table III (see also 'Supplementary Material').

Features of the Kinetic Data for Second-order Rate Law (16)

All previously investigated monotransmetalations of **A** by **C** are irreversible processes with second-order rate law (12) [9]. We now find that reactions of **D** with **C** either obey irreversible second-order rate law (16) or a reversible rate law (17) whose forward component is second-order (see below). The data for all second-order forward processes are collected in Table III.

The second-order rate constants in Tables I and III cover a range of $ca. 3 \times 10^4 \text{ M}^{-1} \text{ s}^{-1}$ at 21°C . The fastest and slowest irreversible reactions at 21°C are **A** ($X = \text{Cl}$) reacting with **C** ($M = \text{Zn}$) (Table I) and **D** ($L = \text{TEED}$, $X = \text{Cl}$) reacting with **C** ($M = \text{Ni}$), respectively, in nitrobenzene (Table III).

Data for Nickel

Second-order rate constants k_{12} and k_{16} for transmetalation by **C** ($M = \text{Ni}$) are similar and not greatly affected by changing the solvent. Changing $X = \text{Cl}$ to Br in **A** or **D** causes only minor rate changes, laws (10) and (15). This indicates that metal- X bond breaking is not a dominant factor in the rate-determining steps of these irreversible reactions of **C**.

Comparison of Data for Cobalt, Nickel and Zinc

Rate constants k_{12} for transmetalation of **A** (Table I) decrease from **C** ($M = \text{Zn}$) to **C** ($M = \text{Ni}$) but there is little effect in changing solvent or $X = \text{Cl}$ to Br . Anticipating the results of the next sections, the rate constants for forward reactions of **D** governed by second-order rate constants k_{16} or k_{17} decrease in the following order: **C** ($M = \text{Cu}$) \approx **B** (Co) $>$ **C** ($M = \text{Ni}$); the high rates for **C** ($M = \text{Cu}$) are unexpected for this highly stable $M(\text{NS})_2$ complex [10] if metal exchange is rate-determining [9]. Notable again is the minor effect of changing solvent or $X = \text{Cl}$ to Br in the reactions of **C** ($M = \text{Ni}$, Cu or Zn) with **A** or **D**; the latter suggests that $M\text{--}X$ bond breaking is not a major factor in any of these second-order forward processes (see below). However, plots of ΔH_{12}^\ddagger versus ΔS_{12}^\ddagger and ΔH_{16}^\ddagger versus ΔS_{16}^\ddagger (not shown) give a common straight line, which suggests similar structural features in the mechanisms of these reactions.

Reversible Reactions of **D** with **B** ($M = \text{Co}$) and **C** ($M = \text{Cu}$) in Nitrobenzene

Without exception, all monotransmetalations of excess copper(II) reactants **A** ($X = \text{Cl}$) with **B** are governed by third-order rate law (10) in methylene chloride or nitrobenzene [9]. The corresponding reactions of **D** with **B** obey third-order rate law (15) except when $M = \text{Co}$ in either solvent; these latter systems are governed by second-order rate law (16), Table III, except when $X = \text{Cl}$ in nitrobenzene, where the observed reaction is reversible.

Without exception, all monotransmetalations of excess **A** ($X = \text{Cl}$ or Br) by **C** are governed by second-order rate law (12) [9]. The corresponding reactions of **D** with **C** obey second-order rate law (16) except when $M = \text{Cu}$ in nitrobenzene, where the observed reaction is reversible. Data which identify specific reversible systems will now be presented.

Reactions of excess **D**, $(2.5\text{--}10.0) \times 10^{-3}$ M, with **B** ($M = \text{Co}$), 2.0×10^{-4} M, and **C** ($M = \text{Cu}$), 1.0×10^{-4} M, were monitored at 625 and 425 nm, respectively, under dinitrogen. Plots of $\ln(A_\infty - A_t)$ versus time were always linear to at least 4 half-lives, indicating a first-order dependence on $[\text{B}]$ or $[\text{C}]$. Plots of the observed pseudo-first-order rate constants at fixed temperature, k_{obs} , versus $[\text{D}]$ were linear but with intercepts on the rate axis,

TABLE IV. Kinetic Data for Reversible Reactions of Excess D with B and C in Nitrobenzene (eqn. (17))

Copper reactant	B or C, M	k_{17}^a	$\Delta H_{17}^\ddagger{}^b$	$\Delta S_{17}^\ddagger{}^c$	k_{17}^d	$\Delta H_{17}^\ddagger{}^b$	$\Delta S_{17}^\ddagger{}^c$	K_{17}^e	$\Delta H_{17}^\ddagger{}^b$	$\Delta S_{17}^\ddagger{}^c$
(TEED) ₂ Cu ₂ Cl ₂	B, Co	370	10.6 ± 0.3	-11 ± 2	0.93	13.3 ± 0.3	-14 ± 1	400	-2.7 ± 0.3	3 ± 2
	C, Cu	1740	11.3 ± 0.4	-5 ± 2	5	11.9 ± 0.4	-15 ± 2	350	-0.6 ± 0.2	10 ± 2
(TEED) ₂ Cu ₂ Br ₂	C, Cu	470	13.9 ± 0.3	1 ± 2	0.83	5.1 ± 0.3	-42 ± 2	560	8.8 ± 0.3	41 ± 2

^aUnits are M⁻¹ s⁻¹ at 21 °C; typical precision ± 5%. ^bUnits are kcal mol⁻¹. ^cUnits are cal deg⁻¹ mol⁻¹ at 25 °C. ^dUnits are s⁻¹ at 21 °C. ^eUnits are M⁻¹ at 21 °C.

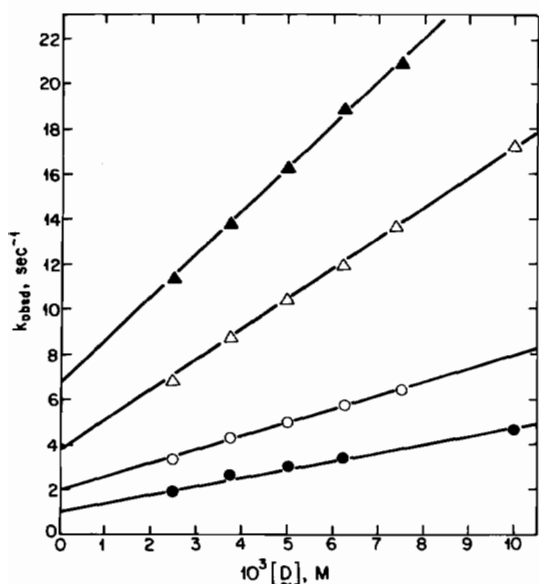


Fig. 5. Plots of k_{obs} (s⁻¹) vs. [D] for the reversible reaction of excess D with B (M = Co) in rate law (17) in nitrobenzene at the following temperatures (°C): ●, 21.8; ○, 31.8; △, 42.3; ▲, 49.8.

indicating rate law (17). Specific examples are shown in Fig. 5 and kinetic data are given in Table IV (see also 'Supplementary Material').

$$\text{rate} = k_{17}[\text{B or C}][\text{D}] + k_{-17} \quad (17)$$

Features of the Kinetics of Reversible Systems

Second-order, forward rate constants k_{17} are not very sensitive to whether the transmetalator is B or C containing M = Co or Cu, and are, in fact, similar to k_{16} for irreversible reactions involving these same reactants (Table III). Reversibility arises from measurable values of k_{-17} , which increases by a factor of about 6 in changing from D (X = Br) to D (X = Cl) reacting with C (M = Cu) in nitrobenzene at 21 °C. Rate constants k_{17} and k_{-17} for reaction of D (X = Cl) with B (M = Co) and C (M = Cu) are quite similar at 21 °C and are higher for more stable C [10]; this indicates that the very different thermodynamic stability [10] of these reagents has little to do with the processes governed

by k_{17} or k_{-17} . However, similar k_{-17} are due to compensated variations in ΔH_{-17}^\ddagger and ΔS_{-17}^\ddagger (Table IV).

The equilibrium constants for the reversible processes, $K_{17} = k_{17}/k_{-17}$, are 430 ± 80 M⁻¹ at 21 °C in nitrobenzene; ΔH_{17} ranges from near zero for D (X = Cl) with C (M = Cu) to 8.6 kcal mol⁻¹ for D (X = Br) with C (M = Cu), and ΔS_{17} ranges from 3–31 cal deg⁻¹ mol⁻¹; the largest ΔH_{17} and ΔS_{17} are observed for D (X = Br) reacting with C (M = Cu).

Before proceeding to a detailed comparison of all the kinetic data and proposed mechanisms for reactions of D with B and C, we wish to emphasize the conditions apparently favoring reversibility, which are (i) reactants D, preferably with X = Cl; most importantly, reversibility was not observed with excess reactant (ENCA)₄Cu₂Cl₂; (ii) solvent nitrobenzene: no reversible systems were detected in methylene chloride; (iii) inert C, best represented by M = Cu, which reacts reversibly with D (X = Cl or Br).

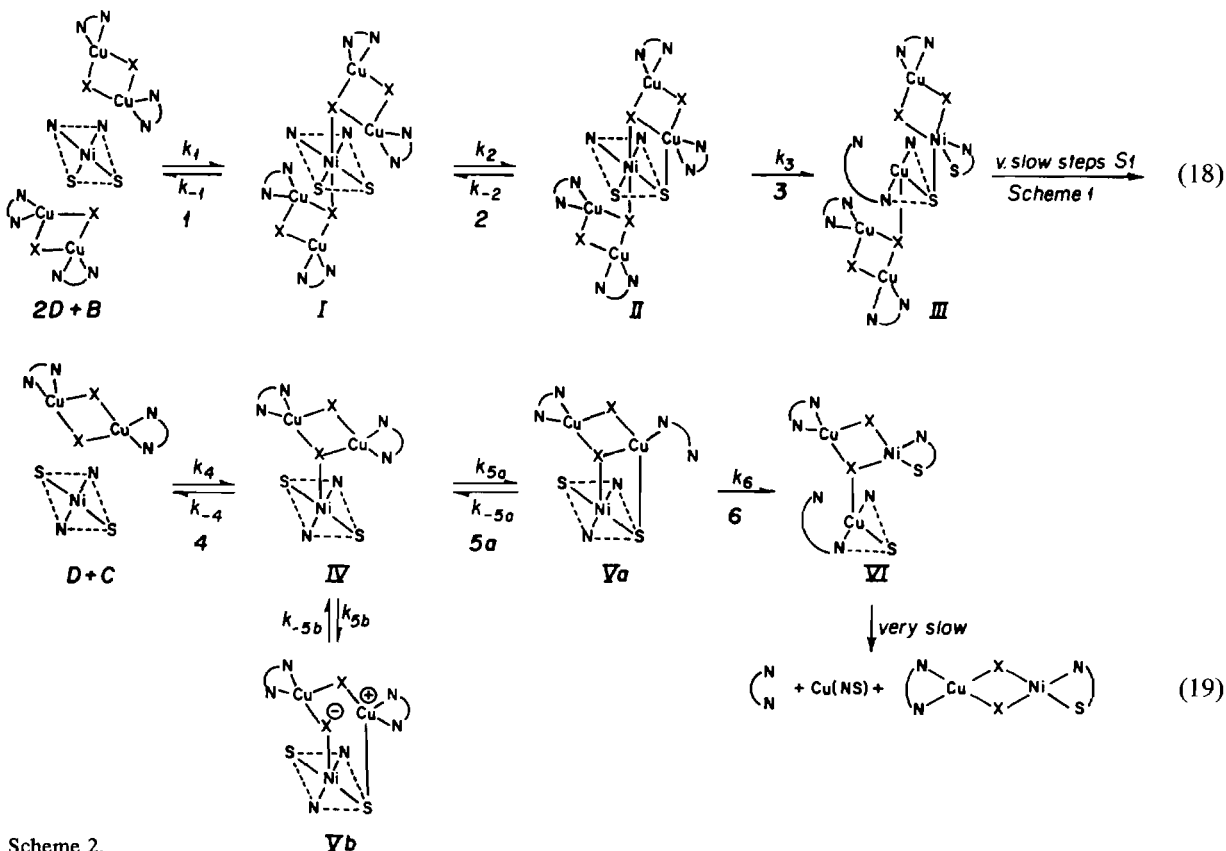
Reaction Mechanisms

We propose the mechanisms of eqns. (18) and (19), Scheme 2, to account for reactions of D and (ENCA)₄Cu₂X₂ with B and C, respectively. Preservation, wherever possible, of four-coordinate copper(I) and an affinity for carbothioate sulfur have been guiding principles in formulating the species proposed.

Irreversible Third-order Systems

Equation (18) is similar to the mechanism proposed [9] to account for the third-order, irreversible monotransmetalation of excess A by B, which also is observed in most cases with excess D (Table II); the Cu–X–Cu connectors are the counterparts of the structural units of A that were used to construct $\bar{\text{C}}\text{u}-\text{X}-\bar{\text{M}}-\bar{\text{S}}$ rings for its transmetalation [9]. Although the molecular geometries of B depend on M [23], that for M = Ni (a flattened tetrahedron with *cis*-carbothioate sulfurs [23]) is shown for simplicity.

The predictive features of eqn. (17) arise from a steady-state treatment of species I and II [9].



If $k_2 \ll k_{-1} \gg k_{-2} \ll k_3$ we obtain eqn. (20), which is of the same form as eqn. (15) and corresponds

$$\text{rate} = K_1 k_2 [\mathbf{B}] [\mathbf{D}]^2 \quad (20)$$

to rate-determining ring-closure step 2 with step 1 ($K_1 = k_1/k_{-1}$) as a rapid pre-equilibrium. As before [9], we adopt these limits because it is known that the formation of bis adducts $\mathbf{B} \cdot \text{py}_2$ is too rapid to measure on the stopped-flow timescale [28]. These circumstances result in $k_{15} = K_1 k_2$, $\Delta H_{15}^\ddagger = \Delta H_1 + \Delta H_2^\ddagger$ and $\Delta S_{15}^\ddagger = \Delta S_1 + \Delta S_2^\ddagger$ in eqn. (20). Rate-determining metal exchange step 3 arises if $k_3 \ll k_{-2}$ and $k_{-1} \ll k_2$ in mechanism (18); these conditions lead to eqn. (21), which has the same form as eqn. (15)

$$\text{rate} = K_1 K_2 k_3 [\mathbf{B}] [\mathbf{D}]^2 \quad (21)$$

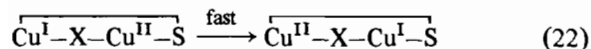
with $k_{15} = K_1 K_2 k_3$, $\Delta H_{15}^\ddagger = \Delta H_1 + \Delta H_2 + \Delta H_3$ and $\Delta S_{15}^\ddagger = \Delta S_1 + \Delta S_2 + \Delta S_3^\ddagger$. As before [9], our task is to try to account for rapid equilibria 1 and 2 in assigning rate-determining steps.

If we again [9] approximate $\Delta S_1 = -44 \text{ cal deg}^{-1} \text{ mol}^{-1}$ for rapid equilibrium step 1, eqn. (18), then rate-determining step 2 predicts $\Delta S_2^\ddagger = \Delta S_{15}^\ddagger + 44 \text{ cal deg}^{-1} \text{ mol}^{-1}$, which ranges from +5 to 67 $\text{cal deg}^{-1} \text{ mol}^{-1}$ and is very positive for most \mathbf{D} systems in Table II. But positive entropies of activation are

not reasonable for ring closure step 2; thus, rate-determining step 3 seems most likely except in the first system of Table II, where ΔS_2^\ddagger is predicted to be 5 $\text{cal deg}^{-1} \text{ mol}^{-1}$ and is within the range observed for rate-determining metal exchange without the broken Cu-X and Cu-N bonds in proposed species **III**. Thus, for the majority of the systems in Table II we assign $\Delta S_{15}^\ddagger = \Delta S_1 + \Delta S_2 + \Delta S_3^\ddagger$, or $\Delta S_3^\ddagger = \Delta S_{15}^\ddagger - \Delta S_1 - \Delta S_2$. If $\Delta S_1 = -44$ [28] and $\Delta S_2 = -10$ (as seems reasonable for step 2), then $\Delta S_3^\ddagger = \Delta S_{15}^\ddagger + 44 + 10 \text{ cal deg}^{-1} \text{ mol}^{-1}$ and 6 of the 7 systems in Table II have rate-determining step 3. In our view the entropy of the activated complex for step 3 depends on the extent of interaction of Cu with X and whether L on Cu is mono- or bidentate: the formulation of **III** in eqn. (18) perhaps corresponds to the highest experimental ΔS_{15}^\ddagger in Table II. The fact that ΔS_{10}^\ddagger (Table I) is always higher than ΔS_{15}^\ddagger (Table II) is consistent with much more facile formation of final products in the transmetalation of **A**, presumably because the copper(II) center in the Cu-X-M-S ring of the analogue of species **II**, eqn. (18), is six-coordinate (ligands X, X, X, μ_4 -O, N, S) [9].

The data for reaction of **D** with **B** ($\text{M} = \text{Cu}$) deserve special attention. How can 'metal exchange' be so rapid that product fragmentation is rate-

determining, particularly when **B** ($M = \text{Cu}$) is such a stable $M(\text{NS})_2$ complex [10]? The probable answer is that 'metal' exchange is very rapid electron-exchange mediated by **X** and/or **S** atoms in Cu-X-Cu-S rings, eqn. (22). This is reasonable because **D** are quite strong reducing agents [20]



and copper has an accessible $M(\text{I})$ state. We also know that electron transfer from copper(I) in $[\text{NCuX}]_4$ to cobalt(III) in $\text{Co}(\text{NS})_3$ precedes metal exchange [8, 10] and that reaction of excess **B** ($M = \text{Cu}$) with **D** rapidly gives 4 mol $\text{Cu}(\text{NS})(\text{s})$ per mol **D** [15]. Electron exchange has the same net result as metal movement in the other systems but is much faster. Little effect of **X** on k_{15} suggests that Cu-X bond-breaking is not part of the activation process for formation of **III**, eqn. (18), with $M = \text{Cu}^{\text{II}}$.

Irreversible Second-order Systems

Equation (19) resembles the mechanism previously proposed for the second-order monotransmetalation of excess **A** by **C** [9] but differs in that it explicitly focusses on the role of bidentate **L** at the site of metal replacement in species **Va** and **Vb**.

We account for irreversible, second-order reactions with rate laws (12) or (16) by setting $k_{5a} \gg k_{5b}$, a condition satisfied by ready ring-opening in **Va** or loss of **N** from the corresponding site in **A**. A steady-state treatment of species **IV** and **Va** with $k_{5a} \ll k_{-4} \gg k_{-5a} \ll k_6$ corresponds to step 5a as the rate-determining step with step 4 ($K_4 = k_4/k_{-4}$) as a rapid pre-equilibrium and leads to eqn. (23), which has the same form as rate law (16). For these conditions $k_{16} = K_4 k_{5a}$, $\Delta H_{16}^\ddagger = \Delta H_4 + \Delta H_{5a}^\ddagger$ and $\Delta S_{16}^\ddagger = \Delta S_4 + \Delta S_{5a}^\ddagger$

$$\text{rate} = K_4 k_{5a} [\text{B or C}] [\text{D}] \quad (23)$$

Alternatively, the conditions $k_6 \ll k_{-5a}$ and $k_{-4} \gg k_{5a}$, which correspond to rate-determining step 6, lead to eqn. (24), which has the same form as eqn. (16) with $k_{16} = K_4 K_{5a} k_6$, $\Delta H_{16}^\ddagger = \Delta H_4 + \Delta H_{5a} + \Delta H_6^\ddagger$ and $\Delta S_{16}^\ddagger = \Delta S_4 + \Delta S_{5a} + \Delta S_6^\ddagger$

$$\text{rate} = K_4 K_5 k_6 [\text{B or C}] [\text{D}] \quad (24)$$

As before [9], we approximate $\Delta S_4 = -25 \pm 3 \text{ cal deg}^{-1} \text{ mol}^{-1}$ from the measured data for $\text{Ni}(\text{NS})_2$ · bipy adduct formation in benzene [28], and put $\Delta S_{5a}^\ddagger = \Delta S_{16}^\ddagger + 25 \text{ cal deg}^{-1} \text{ mol}^{-1}$, which amounts to adding $25 \text{ cal deg}^{-1} \text{ mol}^{-1}$ to ΔS_{16}^\ddagger in Table III. The results range from $\Delta S_{5a}^\ddagger = ca. -10 \text{ cal deg}^{-1} \text{ mol}^{-1}$ to $ca. +60 \text{ cal deg}^{-1} \text{ mol}^{-1}$. The smaller ΔS_{5a}^\ddagger are consistent with rate-determining step 5a, which describes nucleophilic attack of carbothioate **S** to close a Cu-X-M-S ring. In **A** systems this causes

dissociation of monodentate **N** (to preserve five-coordination) and in **D** systems the bidentate ring on the site of attack is opened to counteract the increase of coordination number of copper(I) from 4 to 5. These events would tend to neutralize the entropy decrease anticipated for Cu-X-M-S ring closure.

Some systems in Table III have predicted ΔS^\ddagger which are too positive to be consistent with rate-determining step 5a. In those systems we propose step 6 as rate-determining since its activation entropy would be expected to be positive (ref. 9 and above). Little effect of **X** on k_{16} indicates Cu-S bond breaking as the dominant factor in this process.

Reversible Systems

Species **IV**, eqn. (19), is postulated to have two alternatives, steps 5a or 5b, depending on its constituents and the solvent. In most cases k_{5a} appears to be much greater than k_{5b} , which leads to irreversible rate law (16). In a few systems, however, it appears that $k_{5b} \gg k_{5a}$ and reversible behavior is observed. Although reversible behavior was not observed with **Ni**, we adopt the known square-planar, *trans*-geometry of **C** ($M = \text{Ni}$) [23] for the simplest description of proposed species **Vb**.

Species **Vb** differs from **Va** because of a different result of Cu-X-M-S ring closure, namely the extension or breaking of a X-Cu bond to the site in **D** which is attacked by carbothioate **S**. As a consequence **Vb** is polar, its labelling crudely reflecting the likely charge distribution. This polarity accounts for reversibility only in highly polar nitrobenzene ($\epsilon = 33.5$) [29]. Other attractive features of **Vb** are that metal exchange is retarded because the Cu-X-M-S ring is incomplete and that copper(I) is relatively positive and thus more strongly bound to **X,N,N,S**.

We again adopt step 4 as a rapid pre-equilibrium [28], which gives $k_{17} = K_4 k_{5b}$ and $k_{-17} = k_{-5b}$ in eqn. (19). Thus, $\Delta H_{17}^\ddagger = \Delta H_4 + \Delta H_{5b}^\ddagger$ and $\Delta S_{17}^\ddagger = \Delta S_4 + \Delta S_{5b}^\ddagger$. If $\Delta S_4 = -25 \text{ cal deg}^{-1} \text{ mol}^{-1}$ (ref. 28 and above), then ΔS_{5b}^\ddagger ranges from +11 to +26 $\text{cal deg}^{-1} \text{ mol}^{-1}$ from the data in Table IV, which suggests an 'open' structure with a broken Cu-X bond in the activated complex of step 5b. Since $k_{-17} = k_{-5b}$, we have ΔH_{-5b}^\ddagger ranging from 5.1 to 13.3 kcal mol^{-1} . The ΔS_{-5b}^\ddagger range from -42 to -14 $\text{cal deg}^{-1} \text{ mol}^{-1}$, consistent with reformation of a Cu-X bond in the activated complex for the reverse process. Also, since $\Delta S_{5b} = \Delta S_{17} - \Delta S_4$ we obtain ΔS_{5b} ranging from 28 to 66 $\text{cal deg}^{-1} \text{ mol}^{-1}$, respectively (Table IV), confirming that **Vb** is a highly disordered structure, especially with **D** ($X = \text{Br}$) in association with **C** ($M = \text{Cu}$). Finally, highest ΔH_{17} for $X = \text{Br}$ is quite consistent with required Cu-X bond-breaking in the formation of **Vb**; stronger

Cu–Br than Cu–Cl bonds have been assigned previously (see above and ref. 22).

Reversible Copper Systems

In an earlier section we invoked electron transfer from **D** to **B** ($M = Cu$) to explain rapid step 2 in eqn. (18). This process guarantees irreversibility, a requirement for transmetalation. Therefore, electron transfer cannot be occurring in step 5b for reactions of **C** ($M = Cu$). One possibility is that **C** ($M = Cu$) is a weaker oxidizing agent than **B** ($M = Cu$). Another is that X–Cu bond breaking to give **Vb** is faster than electron transfer in **IV**.

Reaction Precursors

We have been consistent in accounting for rapid precursor formation in **D/B/C** systems with literature data [28]. Therefore, even if the entropy changes applied are grossly in error, the observed activation entropies themselves indicate shifts of rate-determining step, particularly for irreversible reactions of **C** (Table II).

Our earlier work indicated no geometrical factors determining that **B·A₂** are generally more stable than **C·A₂**, despite the fact **B** and **C** ($M = Ni$) are essentially planar while **B** ($M = Co$ or Zn) are tetrahedral [23].

We now find that there are parallels between the behavior of **B** ($M = Ni$ or Cu) reacting with **D** (Table II), which suggests that both **B** are planar and able to form **B·D₂** precursors. However, different, second-order (and sometimes reversible) behavior with **B** ($M = Co$) indicates that its tetrahedral geometry [23] does not allow the formation of even weak complexes **B·D₂** (Table III), while this is not prevented with **A** and is very pronounced for **A** ($X = Br$, Table I). This behavior of **B** ($M = Co$) is clearly due to overriding steric interactions between alkyl substituents in molecules **D** of putative **B·D₂** species. Similar steric interactions also cause large rate variations in the third-order oxidation of **D** by O_2 , eqn. (25) [20], such that construction of an activated complex containing two **D** and

$$d[\text{product}]/dt = k_{40}[\mathbf{D}]^2[\text{O}_2] \quad (25)$$

one O_2 is the rate-determining step under ambient conditions. We also have found that LMX_2 complexes have low affinity for **L** for the same reasons [15].

Thus, although there are many commonalities in the kinetics of monotransmetalation of **A** and **D** by **B** and **C** there are also very significant differences, namely (i) no analogue of rate law (11) in reactions of **D** with **B**; (ii) reversible rate law (17) for reactions of **D** with particular **B** or **C**; and (iii) very slow formation of final $Cu(NS)$ coproducts in transmetalation of **D**.

Transmetalation Selectivity

In a previous paper [10] we concluded from analyses of products from reactions of $[NCuX]_4$ complexes with mixtures of $Co(NS)_3$ and **B** ($M = Co, Ni, Cu, Zn$) that relative transmetalation rates increase with decreasing thermodynamic stability in the order $Cu(NS)_2 \gg Ni(NS)_2 \gg Co(NS)_2 \gg Co(NS)_3 \gg Zn(NS)_2$. The present work suggests that differences of rate law can also affect copper(I) transmetalation selectivity, especially in systems exhibiting reversibility and/or geometric preference.

Supplementary Material

A Table of detailed kinetic data for reactions of **D** with **B** and **C** in aprotic solvents is available from the authors on request. The computer software listings and interfacing schematics are also available from the authors upon request.

Acknowledgements

This work was supported by Grant RR07143 from the Department of Health and Human Services and Grant INT-8512210 from the National Science Foundation, which are gratefully acknowledged. We also thank Mr Adnan Ali and Professor Thomas R. Gilbert for many metal analyses and Mss Noralie Barnett and Betty Cardoza for skilled technical assistance.

References

- 1 N. El-Kady, *Doctoral Dissertation*, Northeastern University, 1986.
- 2 A. El-Toukhy, G.-Z. Cai, G. Davies, T. R. Gilbert, K. D. Onan and M. Veidis, *J. Am. Chem. Soc.*, **106**, 4596 (1984).
- 3 G.-Z. Cai, G. Davies, A. El-Toukhy, T. R. Gilbert and M. Henary, *Inorg. Chem.*, **24**, 1701 (1985).
- 4 G. Davies, M. A. El-Sayed and A. El-Toukhy, *Inorg. Chem.*, **25**, 1925 (1986).
- 5 G. Davies, M. A. El-Sayed, A. El-Toukhy, M. Henary, T. R. Gilbert and K. Nabih, *Inorg. Chem.*, **25**, 1929 (1986).
- 6 G.-Z. Cai, G. Davies, M. A. El-Sayed, A. El-Toukhy and K. D. Onan, *Inorg. Chem.*, **25**, 1935 (1986).
- 7 G. Davies, M. A. El-Sayed and A. El-Toukhy, *Inorg. Chem.*, **25**, 2269 (1986).
- 8 G. Davies, M. A. El-Sayed, A. El-Toukhy, M. Henary and T. R. Gilbert, *Inorg. Chem.*, **25**, 2373 (1986).
- 9 G. Davies, M. A. El-Sayed and A. El-Toukhy, *Inorg. Chem.*, **25**, 3899 (1986).
- 10 G. Davies, M. A. El-Sayed, A. El-Toukhy, M. Henary, T. S. Kasem and C. A. Martin, *Inorg. Chem.*, **25**, 3904 (1986).

- 11 G. Davies, M. A. El-Sayed, A. El-Toukhy, M. Henary and C. A. Martin, *Inorg. Chem.*, **25**, 4479 (1986).
- 12 G. Davies, N. El-Kady, M. A. El-Sayed and A. El-Toukhy, *Inorg. Chim. Acta*, **104**, 131 (1985).
- 13 M. Henary, A. Abu-Raqabah, G. Davies, M. A. El-Sayed and A. El-Toukhy, *Inorg. Chem.*, submitted for publication.
- 14 G. Davies, M. A. El-Sayed, A. El-Toukhy and M. Henary, *Inorg. Chem.*, submitted for publication.
- 15 G. Davies, N. El-Kady, M. A. El-Sayed and A. El-Toukhy, *Inorg. Chim. Acta*, **149**, 21 (1988).
- 16 A. Abu-Raqabah, G. Davies, M. A. El-Sayed, A. El-Toukhy and M. Henary, *Inorg. Chem.*, submitted for publication.
- 17 G. Davies and M. A. El-Sayed, in K. D. Karlin and J. Zubieta (eds.), 'Inorganic and Biochemical Perspectives in Copper Coordination Chemistry', Adenine Press, Guilderland, N.Y., 1983, p. 281.
- 18 M. R. Churchill, G. Davies, M. A. El-Sayed, J. A. Fournier, J. P. Hutchinson and J. A. Zubieta, *Inorg. Chem.*, **23**, 783 (1984).
- 19 (a) D. A. Haitko, *J. Coord. Chem.*, **13**, 119 (1984); (b) D. A. Haitko and M. F. Garbaskas, *Symposium on Inorganic and Biochemical Perspectives in Copper Coordination Chemistry*, Albany, N.Y., July 1984; (c) D. A. Haitko and M. F. Garbaskas, in K. D. Karlin and J. Zubieta (eds.), 'Biological and Inorganic Copper Chemistry', Adenine Press, Guilderland, N.Y., 1986, p. 77, and refs. therein.
- 20 M. A. El-Sayed, A. El-Toukhy and G. Davies, *Inorg. Chem.*, **24**, 3387 (1985).
- 21 R. N. Keller and H. D. Wycoff, *Inorg. Synth.*, **2**, 1 (1946).
- 22 G. Davies and M. A. El-Sayed, *Inorg. Chem.*, **22**, 1257 (1983).
- 23 K. D. Onan, G. Davies, M. A. El-Sayed and A. El-Toukhy, *Inorg. Chim. Acta*, **113**, 109 (1986), and refs. therein.
- 24 G.-Z. Cai, G. Davies, M. A. El-Sayed, A. El-Toukhy and T. R. Gilbert, in K. D. Karlin and J. Zubieta (eds.), 'Biological and Inorganic Copper Chemistry', Adenine Press, Guilderland, N.Y., 1986, p. 115.
- 25 L. El-Sayed, M. F. Iskander, A. El-Toukhy and S. E. Zayan, *Inorg. Chim. Acta*, **6**, 663 (1972).
- 26 M. F. Iskander, L. El-Sayed and A. El-Toukhy, *J. Inorg. Nucl. Chem.*, **42**, 1145 (1980).
- 27 A. El-Toukhy, M. El-Essawi, M. Tawfik, L. El-Sayed and M. F. Iskander, *Transition Met. Chem.*, **8**, 4454 (1983).
- 28 M. F. Iskander, L. El-Sayed, L. Labib and A. El-Toukhy, *Inorg. Chim. Acta*, **86**, 197 (1984); M. F. Iskander, L. El-Sayed, M. Khalil and A. El-Toukhy, *Inorg. Chim. Acta*, **86**, 191 (1984).
- 29 I. A. Koppell and V. A. Palm, in N. B. Chapman and J. Shorter (eds.), 'Advances in Linear Free Energy Relationships', Plenum, London, 1972.